

# Fully gapped $d$ -wave superconductivity in $\text{CeCu}_2\text{Si}_2$

G. M. Pang,<sup>1</sup> M. Smidman,<sup>1</sup> J. L. Zhang,<sup>1</sup> L. Jiao,<sup>1</sup> Z. F. Weng,<sup>1</sup> E. M. Nica,<sup>2,3</sup> Y. Chen,<sup>1</sup> W. B. Jiang,<sup>1</sup> Y. J. Zhang,<sup>1</sup> W. Xie,<sup>1</sup> H. S. Jeevan,<sup>1,4</sup> H. Lee,<sup>1</sup> P. Gegenwart,<sup>5</sup> F. Steglich,<sup>1,6</sup> Q. Si,<sup>2</sup> and H. Q. Yuan<sup>1,7,\*</sup>

<sup>1</sup>Center for Correlated Matter and Department of Physics, Zhejiang University, Hangzhou 310058, China

<sup>2</sup>Department of Physics and Astronomy, Rice University, Houston, Texas 77005, USA

<sup>3</sup>Department of Physics and Astronomy and Quantum Materials Institute, University of British Columbia, Vancouver, B.C., V6T 1Z1, Canada

<sup>4</sup>Experimentalphysik VI, Center for Electronic Correlations and Magnetism, University of Augsburg, 86159 Augsburg, Germany

<sup>5</sup>Experimental Physics VI, Center for Electronic Correlations and Magnetism, University of Augsburg, 86159 Augsburg, Germany

<sup>6</sup>Max Planck Institute for Chemical Physics of Solids, 01187 Dresden, Germany

<sup>7</sup>Collaborative Innovation Center of Advanced Microstructures, Nanjing University, Nanjing 210093, China

The nature of the pairing symmetry of the first heavy fermion superconductor  $\text{CeCu}_2\text{Si}_2$  has recently become the subject of controversy. While  $\text{CeCu}_2\text{Si}_2$  was generally believed to be a  $d$ -wave superconductor, recent low temperature specific heat measurements showed evidence for fully gapped superconductivity, contrary to the nodal behavior inferred from earlier results. Here we report London penetration depth measurements, which also reveal fully gapped behavior at very low temperatures. To explain these seemingly conflicting results, we propose a fully gapped  $d + d$  band-mixing pairing state for  $\text{CeCu}_2\text{Si}_2$ , which yields very good fits to both the superfluid density and specific heat, as well as accounting for a sign change of the superconducting order parameter, as previously concluded from inelastic neutron scattering results.

The structure of the superconducting order parameter has been frequently studied, due to its close relationship with the underlying pairing mechanism. While the conventional electron-phonon pairing mechanism typically leads to  $s$ -wave states with fully opened gaps and a constant sign over the Fermi surface [1], unconventional superconductors with different pairing mechanisms often form states with a sign changing order parameter [2, 3]. For instance, cuprate and many Ce-based heavy fermion superconductors are generally believed to be  $d$ -wave superconductors, with nodal lines in the energy gap on the Fermi surface [4–6]. On the other hand, in the high temperature iron based superconductors, an  $s_{\pm}$ -state has been proposed, with a change of sign of the gap function between disconnected Fermi surface pockets, but the energy gap remains nodeless [7]. In this context, the surprising recent discovery [8–10] of evidence for fully gapped superconductivity in the first heavy fermion superconductor  $\text{CeCu}_2\text{Si}_2$  [11] requires further attention.

Superconductivity in  $\text{CeCu}_2\text{Si}_2$  occurs in close proximity to magnetism. Samples with either superconducting ( $S$ -type), antiferromagnetic ( $A$ -type) or competing phases ( $A/S$ -type) are obtained via slight tuning of the composition within the homogeneity range [12]. High pressure measurements of  $\text{CeCu}_2(\text{Si}_{1-x}\text{Ge}_x)_2$  reveal two distinct superconducting domes, one centered around an antiferromagnetic (AFM) instability at ambient/low pressure, and another near a valence instability at high pressure [13]. The close proximity of superconductivity to an AFM instability suggests that in  $\text{CeCu}_2\text{Si}_2$  it is driven by the corresponding quantum criticality. Inelastic neutron scattering (INS) measurements clearly indicate that the Cooper pairing is associated with a

damped propagating paramagnon mode at the incommensurate ordering wavevector  $\mathbf{Q}_{\text{AF}}$  of the spin-density wave (SDW) order nearby in the phase diagram [14]. The large intensity of the low energy spin excitation spectrum at  $\mathbf{Q}_{\text{AF}}$ , which reveals a spin gap in the superconducting state, as well as a pronounced peak *well inside* the superconducting gap  $2\Delta \approx 5k_B T_c$  [14, 15], implies a sign change of the pairing function between the two regions of the Fermi surface spanned by  $\mathbf{Q}_{\text{AF}}$  [16, 17]. The absence of a coherence peak and the  $\sim T^3$  temperature dependence of the spin-lattice relaxation rate  $[1/T_1(T)]$  in Cu-NQR measured above 100 mK, further suggested an unconventional superconducting order parameter with line nodes in the gap structure [15, 18]. Angle resolved resistivity measurements at 40 mK indicate a four-fold modulation of the upper critical field  $H_{c2}$ , as expected for a  $d$ -wave gap with  $d_{xy}$  symmetry [19], while a sign change spanning  $\mathbf{Q}_{\text{AF}}$  is compatible with  $d_{x^2-y^2}$  pairing symmetry [16]. Therefore,  $\text{CeCu}_2\text{Si}_2$  behaves as an even-parity  $d$ -wave superconductor, whose gap structure has yet to be determined.

However, a recent specific heat investigation reported exponential behavior of  $C(T)/T$  at very low temperatures, suggesting fully gapped superconductivity in  $\text{CeCu}_2\text{Si}_2$  [8]. Following this work, scenarios of multi-band superconductivity with a strong Pauli paramagnetic effect, loop-nodal  $s_{\pm}$  superconductivity, and  $s_{++}$  pairing with no sign change were proposed [9, 10, 20, 21]. Furthermore, scanning tunneling spectroscopy down to 20 mK also hints at a multigap order parameter [22]. Indeed electronic structure calculations reveal that multiple bands cross the Fermi level [8, 23], and renormalized band structure calculations show that the dominant

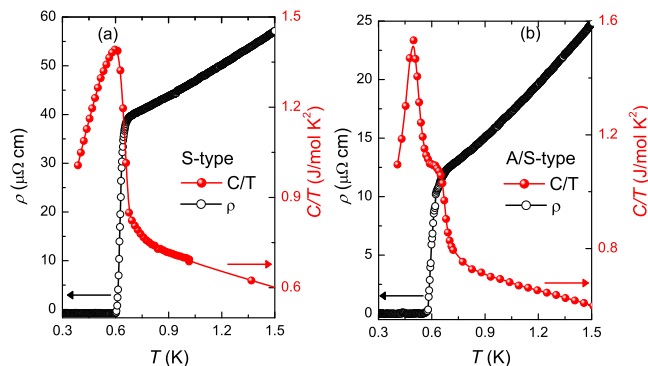


FIG. 1. Specific heat as  $C(T)/T$  and resistivity  $\rho(T)$  of (a)  $S$ -type and (b)  $A/S$ -type  $\text{CeCu}_2\text{Si}_2$ .

heavy band (with  $m^*/m_e \approx 500$ ) leads to Fermi surface sheets mainly consisting of warped cylinders along the  $c$  axis [23]. The aforementioned discrepancies between the pairing symmetries deduced from different measurements show that the superconducting order parameter of  $\text{CeCu}_2\text{Si}_2$  is poorly understood. A particular puzzle is how to reconcile the fully gapped behavior with the previous evidence for a sign changing order parameter and nodal superconductivity. Here we probe the superconducting gap symmetry by measuring the temperature dependence of the London penetration depth, and propose a new scenario of a fully gapped  $d + d$  band-mixing pairing state, which reconciles all the seemingly contradictory results.

## RESULTS

### Resistivity and specific heat

The samples were characterized using resistivity and specific heat measurements, as shown for the  $S$ -type sample in Fig. 1(a). The residual resistivity of the  $S$ -type sample in the normal state just above  $T_c$  is  $\rho_0 \approx 40 \mu\Omega\text{-cm}$ , and a superconducting transition is observed, onseting around 0.65 K and reaching zero resistivity at about 0.6 K. The transition width of  $\approx 0.05$  K is in line with recent reports [19]. The specific heat also shows a superconducting transition with  $T_c \approx 0.64$  K, similar to previous results [8]. The  $A/S$ -type sample [Fig. 1(b)] displays a superconducting transition, onseting around 0.62 K, with a lower residual resistivity of  $\rho_0 \approx 12 \mu\Omega\text{-cm}$ . The specific heat shows both an AFM transition at  $T_N \approx 0.7$  K and a superconducting transition at  $T_c \approx 0.53$  K.

### Temperature dependence of the penetration depth

Measurements of the change of the London penetration depth  $\Delta\lambda(T) = \lambda(T) - \lambda(0)$  for the  $S$ -type sample are displayed in Fig. 2(a). As shown in the inset, a sharp superconducting transition is clearly observed, with an onset at around 0.62 K. To probe the superconducting gap structure, we analyzed the behavior of  $\Delta\lambda(T)$  at low temperatures, and the results are shown in the main panel. The data were fitted with the exponential temperature dependence for a fully-open gap,  $\Delta\lambda(T) = AT^{-\frac{1}{2}}e^{-\Delta(0)/k_B T} + B$ , where  $\Delta(0)$  is the gap magnitude at zero temperature and the constant  $B$  allows for some variation in the extrapolated zero temperature value. The fitting was performed up to 0.12 K ( $\approx T_c/5$ ) and as shown by the solid line in Fig. 2(a), the model can account for the data with a gap of  $\Delta(0) = 0.48k_B T_c$ . A similar gap value of  $\Delta(0) = 0.58k_B T_c$  is obtained from a corresponding fit for the  $A/S$ -type sample, as displayed in the main panel of Fig. 2(b). The small gap values in both cases means that  $\Delta\lambda(T)$  only saturates at very low temperatures. The results indicate similar superconducting properties of the  $S$ - and  $A/S$ -type samples and are consistent with the fully gapped superconductivity reported for an  $S$ -type single crystal in Ref. [8].

The penetration depth of the  $S$ - and  $A/S$ -type samples could also be described by a power law dependence  $\sim T^n$  (*SI Appendix*), with  $n = 2.24$  and 2.43 respectively, when fitting from the base temperature to 0.12 K. For line nodes in the superconducting gap in the presence of impurity scattering,  $\Delta\lambda(T)$  may show quadratic behavior at low temperatures which crosses over to linear behavior at an elevated temperature [24]. To check how the exponent  $n$  evolves with temperature, we also fitted with the power law expression from the base temperature up to a range of temperatures  $T_{up}$ , and the dependence of  $n$  on  $T_{up}$  is shown in the inset of Fig. 2(b). It can clearly be seen that for both samples,  $n$  increases with decreasing  $T_{up}$ , with  $n > 2$ . This indicates that the true low temperature behavior is not a  $\sim T^2$  dependence, as expected for a dirty nodal superconductor, but  $n$  increases as expected for superconductivity exhibiting a full gap. Therefore both the specific heat and  $\Delta\lambda(T)$  data are consistent with fully gapped superconductivity at very low temperatures.

### Analysis of the superfluid density

The superfluid density was calculated using  $\rho_s(T) = [\lambda(0)/\lambda(T)]^2$  and is displayed for both  $S$ - and  $A/S$ -type samples in Fig. 3, where  $\lambda(0) = 2000 \text{ \AA}$  [25]. The superfluid density was fitted following the method of Ref. [26], for a gap  $\Delta_k(T)$  integrated over a cylindrical Fermi surface. The superfluid density data were fitted with an isotropic  $s$ -wave model with a gap  $\Delta(T) =$

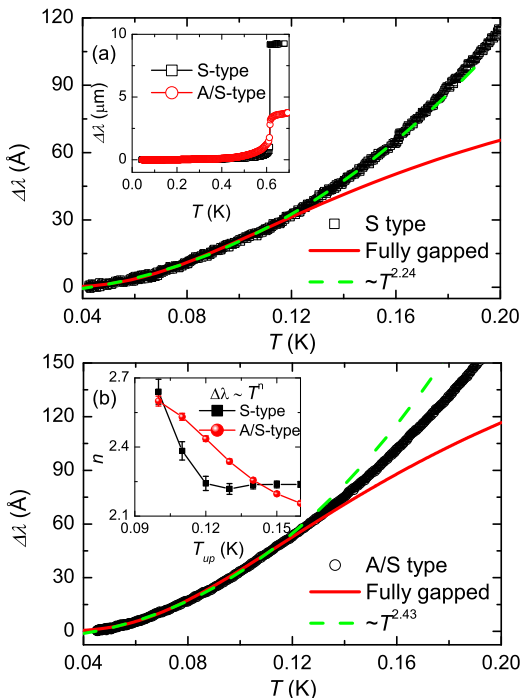


FIG. 2. The change in London penetration depth  $\Delta\lambda(T)$  at low temperature for an (a) *S*-type and (b) *A/S*-type sample of  $\text{CeCu}_2\text{Si}_2$ . The solid lines show fits to a fully gapped model described in the text while the dashed lines show fits to a power law temperature dependence of  $\Delta\lambda(T) \sim T^n$ . The data across the whole temperature range of the superconducting states are displayed in the inset of (a). The inset of (b) shows  $n$  when the data are fitted with  $\Delta\lambda(T) \sim T^n$  up to a temperature  $T_{up}$ .

$\Delta(0)\tanh\left[1.82\left(1.018\left(\frac{T}{T_c}-1\right)\right)^{0.51}\right]$  [27], as well as a *d*-wave model with line nodes ( $\Delta_{\mathbf{k}}(T, \phi) = \Delta(T)\cos 2\phi$ ,  $\phi$ =azimuthal angle). As shown in Fig. 3(a), a single-band isotropic *s*-wave gap cannot account for the data of the *S*-type sample, in contrast to the low temperature  $\Delta\lambda(T)$  data discussed above [Fig. 2(a)]. The single-band *d*-wave model shows reasonable agreement above  $0.5T_c$ , but the agreement is poor at low temperatures, since for this model  $\rho_s(T)$  is linear, but the data are not. The agreement with the *d*-wave model at higher temperatures is consistent with the previously reported evidence for *d*-wave superconductivity. The data were also fitted using a two-gap *s*-wave model [27], and this gives reasonable agreement. The fitted gap values are  $\Delta_1(0) = 1.96k_B T_c$  and  $\Delta_2(0) = 0.75k_B T_c$ , with a fraction for the larger gap of  $x_1 = 0.74$ . Both gap values are slightly larger than the ones obtained for the two-gap model in Ref. [8]. Similarly, neither the *s*- nor *d*-wave single-band models could describe the superfluid density of the *A/S*-type sample at low temperatures [Fig. 3(c)], but the data could be fitted using a two-gap model with  $\Delta_1(0) = 2.0k_B T_c$ ,  $\Delta_2(0) = 0.75k_B T_c$ , and  $x_1 = 0.74$ .

On the other hand, it is difficult to reconcile an *s*-

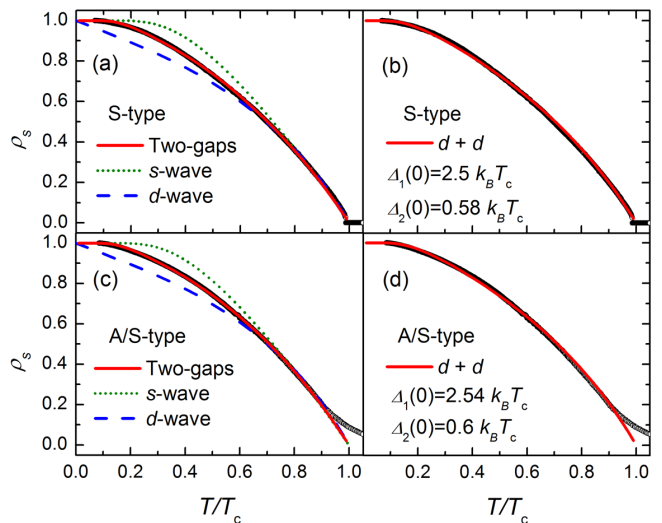


FIG. 3. Superfluid density of  $\text{CeCu}_2\text{Si}_2$  fitted with various models. Fits for the *S*-type sample are shown for (a) two fully-open gaps, as well as *s*- and *d*-wave models denoted by solid, dotted and dashed lines respectively, and (b) a *d + d* band-mixing pairing model. Fits for the *A/S*-type sample are shown for (c) two fully-open gaps, as well as *s*- and *d*-wave models denoted by solid, dotted and dashed lines respectively, and (d) a *d + d* band-mixing pairing model.

wave model with the evidence for a sign changing gap function, as concluded from the inelastic neutron scattering response, where a sharp spin resonance forms at the edge of a spin gap well inside the superconducting gap [14]. Moreover, the incommensurate ordering wave vector of the nearby SDW ( $\mathbf{Q}_{\text{AF}}$ ) is identical to the nesting wave vector spanning the flat parallel parts of the warped cylinders [28]. This shows that there is a sign change of the pair wave function inside the dominating heavy-fermion band, which is incompatible with a nodeless  $s_{\pm}$  pairing state [21]. On the other hand, if there is no sign change of the gap function across the Fermi surface,  $\Delta_{\mathbf{k}}\Delta_{\mathbf{k}+\mathbf{q}} = |\Delta_{\mathbf{k}}||\Delta_{\mathbf{k}+\mathbf{q}}|$ , the coherence factor in the spin susceptibility  $\chi''(\mathbf{q}, \omega)$  is vanishingly small [29, 30]. Consequently, in this case, the spin spectrum will not have a sharp peak, although there may be a broad enhancement of the spectral weight above  $2\Delta$  [31]. However, when there is a change of sign of the gap function between regions of the Fermi surface connected by  $\mathbf{q} = \mathbf{Q}_{\text{AF}}$ , there is an enhanced coherence factor since  $\Delta_{\mathbf{k}}\Delta_{\mathbf{k}+\mathbf{q}} = -|\Delta_{\mathbf{k}}||\Delta_{\mathbf{k}+\mathbf{q}}|$ . This gives rise to a sharp peak in  $\chi''(\mathbf{q}, \omega)$  below  $2\Delta$ , leading to the conclusion that there must be a sign changing order parameter in  $\text{CeCu}_2\text{Si}_2$  [16, 17]. By a similar argument, the lack of a coherence peak in NQR measurements also strongly disfavors superconductivity without a sign reversal [15, 18, 32]. Furthermore, given the strong Coulomb repulsion in *Ce*-based heavy fermion superconductors, the order parameter must be anisotropic with a sign change, without run-

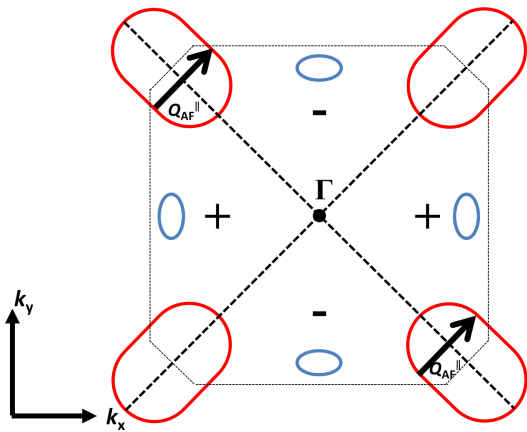


FIG. 4. An illustration of the warped parts of the cylindrical Fermi surfaces (red) in  $\text{CeCu}_2\text{Si}_2$  at particular values of  $k_z$ , corresponding to the nesting portions of the three-dimensional Fermi surface, as well as additional smaller pockets (blue) projected onto the  $k_x - k_y$  wavevector plane [23]. The component  $Q_{\text{AF}}^{\parallel}$  of the antiferromagnetic wavevector  $Q_{\text{AF}}$  projected into the same wavevector plane connects the parts of the heavy Fermi surface with a sign change in the intraband pairing component. The corresponding Fermi surface and nesting wavevector  $\tau = Q_{\text{AF}}$  in the three-dimensional space are those displayed in Fig. 3(b) of Ref. [28].

ning into the issue of a large  $\mu^*$  [33]. In other words, the  $f$ -electrons have a Coulomb repulsion that is much larger than their effective Fermi energy, and they must avoid each other, thereby excluding any sign-preserving pairing function. In such strongly correlated superconductors, even anisotropic and sign-changing pairing states can be robust against disorder [33]. Indeed, potential scattering (due to a site exchange between Cu and Si of less than 1% within the homogeneity range [34]) which enhances the residual resistivity by a factor of  $\approx 4$ , apparently has an almost negligible influence on  $T_c$ , cf. the resistivity results on the  $S$ - and  $A/S$ -samples in Figs. 1(a) and (b). Also, recent experiments on electron-irradiated samples revealed only a minor change of  $T_c$  [9]. At the same time, just like in the cuprates, the effect of substitutional disorder on  $T_c$  is known to be site and size dependent [35]. For  $\text{CeCu}_2\text{Si}_2$ , the superconducting  $T_c$  was found to be extremely sensitive to non-magnetic substitutions on the Cu site: for example, Rh, Pd, and Mn substitution for Cu at a level of  $\approx 1$  at% fully suppresses superconductivity [35], which is impossible to account for in the scenario of an  $s$ -wave state without a sign change of the order parameter. Further studies are needed to develop a detailed understanding of all these observations.

In the present work, we consider a pairing function which, by analogy with an  $s\tau_3$  pairing state [36], has an effective gap as a result of intraband pairing with  $d_{x^2-y^2}$  symmetry and interband pairing with  $d_{xy}$  symmetry; our pairing function preserves both the fully gapped nature and order parameter sign change along  $Q_{\text{AF}}$  on a single

nested Fermi surface. The  $s\tau_3$  pairing state was introduced in the context of the iron-based superconductors (*SI Appendix*) [36], as part of the studies about orbital-selective superconducting pairing [37–40]. There, the pairing function has the form  $\Delta \sim s_{x^2y^2}(\mathbf{k}) \times \tau_3$  (“ $s\tau_3$ ”), as a product of an  $s$ -wave form factor and a Pauli matrix in the  $d_{xz}, d_{yz}$  orbital sub-space. For that case, the inter-orbital mixing in the dispersion part of the Hamiltonian ensures that in the *band basis* the pairing is equivalent to a superposition of intra- and inter-band components with  $d_{x^2-y^2}(\mathbf{k})$  and  $d_{xy}(\mathbf{k})$  form factors respectively. The resulting quasiparticle spectrum acquires a non-vanishing  $|\Delta(\mathbf{k})|^2$  contribution, as the two components are added in quadrature, ensuring a full gap on the whole Fermi surface with a sign change of the intraband component of the gap function. It is also shown how this pairing channel can be stabilized within a self-consistent five-orbital model, with a full gap and a resonance in the spin-excitation spectrum. Similar to the case considered in Ref. [36],  $Q_{\text{AF}}$  of  $\text{CeCu}_2\text{Si}_2$  will connect two parts of the Fermi surface with a sign change in the intraband component of the gap function (see Fig. 4), thereby generating an enhanced spin spectral weight just above a threshold energy  $E_0 = 3.9k_B T_c$  [14], inside the superconducting gap  $2\Delta_1 \approx 5 k_B T_c$ , see below and [15].

In the following, we apply a simplified model for the gap structure to  $\text{CeCu}_2\text{Si}_2$ , given by summing contributions from the two  $d$ -wave states in quadrature, with  $\Delta(T, \phi) = [(\Delta_1(0)\cos(2\phi))^2 + (\Delta_2(0)\sin(2\phi))^2]^{\frac{1}{2}}\delta(T)$ , where  $\delta(T)$  is the gap temperature dependence from Bardeen-Cooper-Schrieffer theory [1], which we used previously. In general, a  $d+d$  band-mixing pairing can introduce corrections to the gap given above, due to the non-degeneracy of the bands throughout the Brillouin zone, which would then lead to an extra parameter, the band splitting. In the following, we will show that the data can be well fit by the simple function without this extra parameter. Although the  $d_{xy}$  and  $d_{x^2-y^2}$  states each have two line nodes, the nodes of the two states are offset by  $\pi/4$  in the  $k_x - k_y$  plane and as a result, the gap function is nodeless everywhere on a cylindrical Fermi surface. It should also be noted that for this model the same  $\rho_s(T)$  is calculated upon exchanging  $\Delta_1(0)$  and  $\Delta_2(0)$ . The superfluid density of the  $S$ -type sample was fitted using this model and the results are shown in Fig. 3(b). It can be seen that such a model can also fit the data well, with gap parameters of  $\Delta_1(0) = 2.5k_B T_c$  and  $\Delta_2(0) = 0.58k_B T_c$ . In Fig. 3(d),  $\rho_s(T)$  for the  $A/S$ -type sample is equally well fitted, with similar parameters of  $\Delta_1(0) = 2.54k_B T_c$  and  $\Delta_2(0) = 0.6k_B T_c$ . The values of the larger gap agree almost perfectly with the gap value obtained from Cu-NQR measurements at higher temperatures [15]. Furthermore, this model only uses two fitting parameters, while the two band  $s$ -wave model of Ref. [8] needs three.

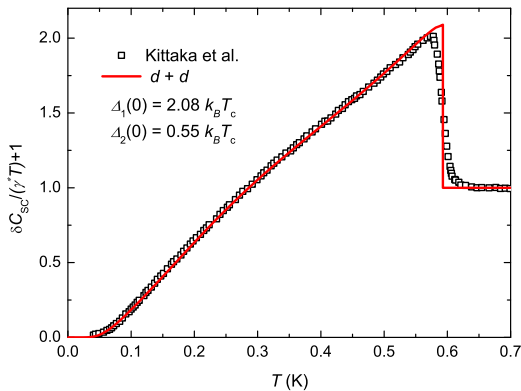


FIG. 5. Specific heat of  $S$ -type  $\text{CeCu}_2\text{Si}_2$  digitized from Ref. [8]. The solid line shows a fit to the  $d+d$  band-mixing pairing model.

### Analysis of the temperature dependence of the specific heat

We also reanalyzed the specific heat data digitized from Ref. [8] using the  $d+d$  band-mixing pairing model. As shown in Fig. 5, the data can also be well described using this model, with fitted parameters  $\Delta_1(0) = 2.08 k_B T_c$  and  $\Delta_2(0) = 0.55 k_B T_c$ . The value of the small gap is similar to that obtained from the superfluid density fit, while the large gap is smaller in comparison. It should be noted that the calculated superfluid density requires an estimation of  $G/\lambda(0)$ , where  $G$  is a calibration constant for the TDO method, and the small differences in the gap values from the fits may arise due to uncertainties in this value.

## DISCUSSION AND SUMMARY

Both the superfluid density and specific heat results are highly consistent with a model of the  $d+d$  band-mixing pairing state, which most importantly also explains the sign change of the superconducting order parameter. Although the fully gapped nature of the pairing state means that the density of states  $N(E)$  is zero at low energies,  $N(E)$  is nearly linear above the small gap, much like for pairing states with line nodes. This is also consistent with the literature results showing  $d$ -wave superconductivity [15, 18], which were not obtained at low enough temperatures to observe clear evidence for fully gapped behavior. The lack of a coherence peak below  $T_c$  in the Cu-NQR  $1/T_1(T)$  measurements [15, 18, 32] can also not be accounted for by a two-gap  $s$ -wave model, but is readily taken into account by the anisotropic  $d+d$  state, which changes sign along  $\mathbf{Q}_{\text{AF}}$  across the Fermi surface. We note that the effective gap corresponding to a  $d+d$  band-mixing pairing is formally identical to one obtained from a  $d+id$  pairing and the good fits

to  $\rho_s(T)$  and the specific heat are also consistent with this pairing. In the  $d+id$  state, time-reversal symmetry would be broken and although no clear experimental indication of a time-reversal symmetry breaking superconducting state was found from  $\mu\text{SR}$  measurements of  $A/S$  type samples [41], this requires further study. By contrast, a  $d+d$  band-mixing pairing is invariant under time-reversal, while generating the expected sign-change.

From a theoretical perspective, unconventional superconductors in the presence of strong correlations are generally expected to be robust against disorder [33]. This has been demonstrated in models for strongly correlated superconductivity driven by short-range spin-exchange interactions [42, 43]. The  $s\tau_3$  pairing state [36] arises in a similar fashion, and is also expected to be robust against disorder. Because the  $4f$ -electrons in heavy fermion systems undoubtedly have strong correlations, the  $d+d$  band-mixing pairing state proposed for  $\text{CeCu}_2\text{Si}_2$  should be similarly robust to disorder, except for atomic substitutions [35, 44].

In conclusion, we have studied the change of penetration depth  $\Delta\lambda(T)$  and normalized superfluid density  $\rho_s(T)$  of the heavy fermion superconductor  $\text{CeCu}_2\text{Si}_2$  (both  $A/S$ - and  $S$ - type samples). The behavior of  $\Delta\lambda(T)$  at very low temperatures agrees with fully gapped superconductivity, as concluded from specific heat measurements [8]. We demonstrate that a nodeless  $d+d$  band-mixing pairing state can account for the temperature dependence of both the superfluid density and specific heat. This state has the necessary sign change of the superconducting order parameter along  $\mathbf{Q}_{\text{AF}}$  on the heavy Fermi surface deduced from INS [14], and is consistent with the lack of a coherence peak in  $1/T_1(T)$ . The model also explains the consistency of  $d$ -wave superconductivity at higher temperatures, previously reported from  $1/T_1(T)$  measurements [15, 18, 32]. We therefore propose this  $d+d$  band-mixing pairing state to be the superconducting order parameter of  $\text{CeCu}_2\text{Si}_2$ . Given that this is also a strong candidate pairing state for FeSe based superconductors [36], such a pairing model may well be applicable to a wider range of fully gapped unconventional superconductors, including the case of a single  $\text{CuO}_2$  layer [45].

## METHODS

$\text{CeCu}_2\text{Si}_2$  single crystals were synthesized by a modified Bridgman technique using a self-flux method [46]. The temperature dependence of the London penetration depth shift  $\Delta\lambda(T) = G\Delta f(T)$  was measured down to about 40 mK using a tunnel diode oscillator (TDO) based technique [47], where  $\Delta f(T) = f(T) - f(0)$ ,  $f(T)$  is the resonant frequency of the TDO coil, and  $G$  is a calibration constant [48].

## ACKNOWLEDGMENTS

We would like to thank R. Yu, S. Kirchner, G. Zwicknagl, P. Coleman, D. J. Scalapino, O. Stockert, S. Kittaka, and M. B. Salamon for valuable discussions. The work at Zhejiang University has been supported by the National Key R&D Program of China (Grants No. 2017YFA0303100 and No. 2016YFA0300202), National Natural Science Foundation of China (U1632275, 1147425, and 11604291) and the Science Challenge Project of China (Project No. TZ2016004). The work at Rice University has been supported by the NSF Grant No. DMR-1611392, the Robert A. Welch Foundation Grant No. C-1411, a QuantEmX grant from the Institute for Complex Adaptive Matter (ICAM) and the Gordon and Betty Moore Foundation through Grant No. GBMF5305 (Q.S.), and the Center for Integrated Nanotechnologies, a U.S. DOE Basic Energy Sciences (BES) user facility. The work is also supported by the Sino-German Cooperation Group on Emergent Correlated Materials (GZ1123). Q.S. acknowledges the hospitality of the Aspen Center for Physics (NSF grant No. PHY-1607611) and the University of California, Berkeley.

## AUTHOR CONTRIBUTIONS

The project was designed by H.Q.Y.. The crystals were grown by H.S.J., Y.J.Z. W.X., H.L., and P.G.. G.M.P., M.S., J.L.Z., L.J., Z.F.W., Y.C., W.B.J. and H.Q.Y. performed the measurements, which were analyzed by G.M.P., M.S., F.S. and H.Q.Y. based on the theoretical model conceived by E.M.N. and Q.S.. The manuscript was written by G.M.P, M.S, F.S., J.L., Q.S. and H.Q.Y.

---

\* hqyuan@zju.edu.cn

- [1] Bardeen J, Cooper LN, Schrieffer JR (1957) Theory of superconductivity. *Physical Review* 108:1157-1204.
- [2] Anderson PW (2007) Is there glue in cuprate superconductors? *Science* 316:1705-1707.
- [3] Scalapino DJ (2012) A common thread: The pairing interaction for unconventional superconductors. *Rev Mod Phys* 84:1383-1417.
- [4] Kotliar G, Liu J (1988) Superexchange mechanism and  $d$ -wave superconductivity. *Phys Rev B* 38:5142-5145(R).
- [5] Sigrist M, Ueda K (2001) Phenomenological theory of unconventional superconductivity. *Rev Mod Phys* 63:239-311.
- [6] Movshovich R, Jaime M, Thompson JD, Petrovic C, Fisk Z, Pagliuso PG, Sarrao JL (2001) Unconventional superconductivity in CeIrIn<sub>5</sub> and CeCoIn<sub>5</sub>: specific heat and thermal conductivity studies. *Phys Rev Lett* 86:5152-5155.
- [7] Wang F, Lee D-H (2011) The electron-pairing mechanism of iron-based superconductors. *Science* 332:200-204.
- [8] Kittaka S, Aoki Y, Shimura Y, Sakakibara T, Seiro S, Geibel C, Steglich F, Ikeda H, Machida K (2014) Multiband superconductivity with unexpected deficiency of nodal quasiparticles in CeCu<sub>2</sub>Si<sub>2</sub>. *Phys Rev Lett* 112:067002.
- [9] Yamashita T, Takenaka T, Tokiwa Y, Wilcox JA, Mizukami Y, Terazawa D, Kasahara Y, Kittaka S, Sakakibara T, Konczykowski M, Seiro S, Jeevan HS, Geibel C, Putzke C, Onishi T, Ikeda H, Carrington A, Shibauchi T, Matsuda Y (2017) Fully gapped superconductivity with no sign change in the prototypical heavy-fermion CeCu<sub>2</sub>Si<sub>2</sub>. *Sci Adv* 3:e1601667.
- [10] Takenaka T, Mizukami Y, Wilcox JA, Konczykowski M, Seiro S, Geibel C, Tokiwa T, Kasahara Y, Putzke C, Matsuda Y, Carrington A, Shibauchi T (2017) Full-gap superconductivity robust against disorder in heavy-fermion CeCu<sub>2</sub>Si<sub>2</sub>. *Phys Rev Lett* 119:077001.
- [11] Steglich F, Aarts J, Bredl CD, Lieke W, Meschede D, Franz W, Schäfer H (1979) Superconductivity in the presence of strong Pauli paramagnetism: CeCu<sub>2</sub>Si<sub>2</sub>. *Phys Rev Lett* 43:1892-1896.
- [12] Steglich F, Gegenwart P, Geibel C, Helfrich R, Hellmann P, Lang M, Link A, Modler R, Sparn G, Büttgen N, Loidl A (1996) New observations concerning magnetism and superconductivity in heavy-fermion metals. *Physica B : Condensed Matter* 223:1-8.
- [13] Yuan HQ, Grosche FM, Deppe M, Geibel C, Sparn G, Steglich F (2003) Observation of two distinct superconducting phases in CeCu<sub>2</sub>Si<sub>2</sub>. *Science* 302:2104-2107.
- [14] Stockert O, Arndt J, Faulhaber E, Geibel C, Jeevan HS, Kirchner S, Loewenhaupt M, Schmalzl K, Schmidt W, Si Q, Steglich F (2011) Magnetically driven superconductivity in CeCu<sub>2</sub>Si<sub>2</sub>. *Nature Physics* 7:119-124.
- [15] Fujiwara K, Hata Y, Kobayashi K, Miyoshi K, Takeuchi J, Shimaoka Y, Kotegawa H, Kobayashi TC, Geibel C, Steglich F (2008) High pressure NQR measurement in CeCu<sub>2</sub>Si<sub>2</sub> up to sudden disappearance of superconductivity. *J Phys Soc Jpn* 77:123711.
- [16] Eremin I, Zwicknagl G, Thalmeier P, Fulde P (2008) Feedback spin resonance in superconducting CeCu<sub>2</sub>Si<sub>2</sub> and CeCoIn<sub>5</sub>. *Phys Rev Lett* 101:187001.
- [17] Bernhoeft N (2000) Superconductor order parameter symmetry in UPd<sub>2</sub>Al<sub>3</sub>. *Eur Phys J B* 13:685-694.
- [18] Ishida K, Kawasaki Y, Tabuchi K, Kashima K, Kitaoka Y, Asayama K, Geibel C, Steglich F (1999) Evolution from magnetism to unconventional superconductivity in a series of Ce<sub>x</sub>Cu<sub>2</sub>Si<sub>2</sub> compounds probed by Cu NQR. *Phys Rev Lett* 82:5353-5356.
- [19] Vieyra HA, Oeschler N, Seiro S, Jeevan HS, Geibel C, Parker D, Steglich F (2011) Determination of gap symmetry from angle-dependent  $H_{c2}$  measurements on CeCu<sub>2</sub>Si<sub>2</sub>. *Phys Rev Lett* 106:207001.
- [20] Tsutsumi Y, Machida K, Ichioka M (2015) Hidden crossover phenomena in strongly Pauli-limited multiband superconductors: Application to CeCu<sub>2</sub>Si<sub>2</sub>. *Phys Rev B* 92:020502(R).
- [21] Ikeda H, Suzuki M, Arita R (2015) Emergent loop-nodal  $s\pm$ -Wave superconductivity in CeCu<sub>2</sub>Si<sub>2</sub>: similarities to the iron-based superconductors. *Phys Rev Lett* 114:147003.
- [22] Enayat M, Sun Z, Maldonado A, Suderow H, Seiro S, Geibel C, Wirth S, Steglich F, Wahl P (2016) Super-

- conducting gap and vortex lattice of the heavy fermion compound  $\text{CeCu}_2\text{Si}_2$ . *Phys Rev B* 93:045123.
- [23] Zwicknagl G, Pulst U (1993)  $\text{CeCu}_2\text{Si}_2$ : Renormalized band structure, quasiparticles and co-operative phenomena. *Physica B* 895:186-188.
- [24] Hirschfeld PJ, Goldenfeld N (1993) Effect of strong scattering on the low-temperature penetration depth of a  $d$ -wave superconductor. *Phys Rev B* 48:4219-4222.
- [25] Rauchschwalbe U, Lieke W, Bredl CD, Steglich F, Aarts J, Martini KM, Mota AC (1982) Critical fields of the “heavy-fermion” superconductor  $\text{CeCu}_2\text{Si}_2$ . *Phys Rev Lett* 49:1448-1451.
- [26] Prozorov R, Giannetta RW (2006) Magnetic penetration depth in unconventional superconductors. *Supercond Sci Technol* 19:R41-R67.
- [27] Carrington A, Manzano F (2003) Magnetic penetration depth of  $\text{MgB}_2$ . *Physica C* 385:205-214.
- [28] Stockert, O, Faulhaber E, Zwicknagl G, Stüßer N, Jeevan HS, Deppe M, Borth R, KÜchler R, Loewenhaupt M, Geibel C, Steglich F (2004) Nature of the  $A$  phase in  $\text{CeCu}_2\text{Si}_2$ . *Phys Rev Lett* 92:136401.
- [29] Fong HF, Keimer B, Anderson PW, Reznik D, Dogan F, Aksay IA (1995) Phonon and magnetic neutron scattering at 41 meV in  $\text{YBa}_2\text{Cu}_3\text{O}_7$ . *Phys Rev Lett* 75:316-319.
- [30] Eschrig M (2006) The effect of collective spin-1 excitations on electronic spectra in high- $T_c$  superconductors. *Adv Phys* 55:47-183.
- [31] Onari S, Kontani H, Sato M (2010) Structure of neutron-scattering peaks in both  $s_{++}$ -wave and  $s_{\pm}$ -wave states of an iron pnictide superconductor. *Phys Rev B* 81:060504(R).
- [32] Kitagawa S, Higuchi T, Manago M, Yamanaka T, Ishida K, Jeevan HS, Geibel C (2017) Magnetic and superconducting properties of an  $S$ -type single-crystal  $\text{CeCu}_2\text{Si}_2$  probed by  $^{63}\text{Cu}$  nuclear magnetic resonance and nuclear quadrupole resonance. *Phys Rev B* 96:134506.
- [33] Anderson PW (1997) *The theory of superconductivity in the high  $T_c$  cuprate superconductors*. Princeton University Press.
- [34] Steglich F, Gegenwart P, Geibel C, Hinze P, Lang M, Langhammer C, Sparn G, Tayama T, Trovarelli O, Sato N, Dahm T and Varelogiannis T (2001) in *More is Different - Fifty years of condensed matter physics*, eds Phuan Ong N, Bhatt P, Princeton University Press, pp 191.
- [35] Spille H, Rauchschwalbe U, Steglich F (1983) Superconductivity in  $\text{CeCu}_2\text{Si}_2$ : Dependence of  $T_c$  on alloying and stoichiometry. *Helv Phys Acta* 56:165-177.
- [36] Nica EM, Yu R, Si Q (2017) Orbital selective pairing and superconductivity in iron selenides. *npj Quantum Materials* 2:24.
- [37] Goswami P, Nikolic P, Si Q (2010) Superconductivity in multi-orbital  $t - J_1 - J_2$  model and its implications for iron pnictides. *Europhys. Lett.* 91:37006.
- [38] Yu R, Zhu JX, Si Q (2014) Orbital-selective superconductivity, gap anisotropy and spin resonance excitations in a multiorbital  $t$ - $J_1$ - $J_2$  model for iron pnictides. *Phys. Rev. B* 89:024509.
- [39] Ong TT, Coleman P (2013) Tetrahedral and orbital pairing: a fully gapped pairing scenario for the iron-based superconductors. *Phys. Rev. Lett.* 111:217003.
- [40] Ong T, Coleman P, Schmalian J (2016) Entangled Orbital Triplets: hidden  $d$ -wave Cooper pairs of  $s$  pairing. *Proc. Nat. Acad. Sci* 113:5486-5491.
- [41] Feyerherm R, Amato A, Geibel C, Gygax FN, Hellmann P, Heffner RH, MacLaughlin DE, Müller-Reisener R, Nieuwenhuys GJ, Schenck A, Steglich F (1997) Competition between magnetism and superconductivity in  $\text{CeCu}_2\text{Si}_2$ . *Phys Rev B* 56:699-710.
- [42] Chakraborty D, Kaushal N, Ghosal A (2017) Pairing theory for strongly correlated  $d$ -wave superconductors. *Phys. Rev. B* 96:134518.
- [43] Garg A, Randeria M, Trivedi N (2008) Strong correlations make high-temperature superconductors robust against disorder. *Nat. Phys.* 4:762.
- [44] Alloul H, Bobroff J, Gabay M, Hirschfeld PJ (2009) Defects in correlated metals and superconductors. *Rev Mod Phys* 81:45108.
- [45] Zhong Y, Wang Y, Han S, Lv YF, Wang WL, Zhang D, Ding H, Zhang YM, Wang LL, He K, Zhong RD, Schneeloch John A., Gu GD, Song CL, Ma XC, Xue QK (2016) Nodeless pairing in superconducting copper-oxide monolayer films on  $\text{Bi}_2\text{Sr}_2\text{CaCu}_2\text{O}_{8+\delta}$ . *Sci Bull* 61:1239-1247.
- [46] Seiro S, Deppe M, Jeevan H, Burkhardt U, Geibel C (2010) Flux crystal growth of  $\text{CeCu}_2\text{Si}_2$ : Revealing the effect of composition. *physica status solidi (b)* 247:614-616.
- [47] Van Degrift CT (1975) Tunnel diode oscillator for 0.001 ppm measurements at low temperatures. *Rev Sci Instrum* 46:599-607.
- [48] Prozorov R, Giannetta RW, Carrington A, Araujo-Moreira FM (2000) Meissner-London state in superconductors of rectangular cross section in a perpendicular magnetic field. *Phys Rev B* 62:115-118.

# Supporting information

## Theory of the $d+d$ pairing

*A priori*, the  $d+d$  multiband pairing functions used in the analysis described in the main text can (i) produce a full gap along the Fermi pockets illustrated in Fig. 4 (main text) and (ii) introduce a sign change between regions of the Fermi surface connected by the antiferromagnetic wavevector  $\mathbf{Q}_{AF}$  and hence allow for the presence of an in-gap (below  $2\Delta$ ) peak in the dynamical spin susceptibility. Reconciling points (i) and (ii) is crucial for any proposed pairing, as indicated by the experiments discussed in the main text. This pairing function has clear conceptual advantages over the more conventional single and two  $s$ -wave gaps or the single  $d$ -wave gap, all of which are also minimal and phenomenological, but have difficulty allowing for *both* requirements (i) and (ii).

A pairing of multiband  $d+d$  type was initially proposed in Ref. 36 by two of the authors, in the context of similar experimental results for Fe-chalcogenide superconductors (SC). In view of the availability of detailed effective tight-binding models and of well-established orbital-dependent correlations in that case, the pairing was introduced in an orbital basis. Dubbed an “ $s\tau_3$ ” pairing, it consisted of the direct product of an  $s$ -wave form factor and a Pauli matrix  $\tau_3$  in the space of  $3d_{xz}$  and  $3d_{yz}$  orbitals, which altogether change sign under a  $\pi/4$  rotation in the Brillouin zone (an irreducible  $B_{1g}$  representation of the  $D_{4h}$  point group). One of the essential aspects was that in a well-defined, minimal two-orbital model, the non-interacting band part and the pairing matrices do not commute. In an equivalent band basis, this results in *both intra- and inter-band* pairing components, which are associated with  $d_{x^2-y^2}(\mathbf{k})$  and  $d_{xy}(\mathbf{k})$  form factors respectively:

$$\Delta(\mathbf{k}) = \Delta_1(\mathbf{k})[d_{x^2-y^2}] \alpha_3 + \Delta_2(\mathbf{k})[d_{xy}] \alpha_1. \quad (\text{S1})$$

where  $\alpha_3$  and  $\alpha_1$  are Pauli matrices in *band* space. The intra-band pairing, denoted by  $\alpha_3$ , must vanish along the diagonals of the BZ, while the inter-band pairing, marked by  $\alpha_1$ , vanishes along the axes. Crucially, *both components cannot vanish simultaneously*, excluding the zeroes of a common  $s$ -wave form factor. As an important consequence, the gap is essentially given by the quadrature of the two components and is finite throughout the FS. The situation in this case is illustrated by Fig. 1 in Ref. 36.

While the two-orbital model allows for analytical studies of the gap structure and excitation spectra, the  $s\tau_3$  pairing is readily generalized to more complex cases. Indeed, in a more realistic five-orbital model for the Fe-chalcogenides, it was shown in Ref. 36 that the properties i) and ii) stated above are the robust characteristics of the pairing state.

While the analysis of a  $d+d$  multiband pairing function in the case of the Fe-based SC was greatly aided by the availability of established models, the essential insight into the advantages of minimal two-band  $d+d$  pairing can be readily generalized to other SCs and to  $\text{CeCu}_2\text{Si}_2$  in particular, on a phenomenological basis. In this case, we propose a two-band minimal pairing matrix which parallels (S1) but simplifies  $\Delta_1(\mathbf{k})[d_{x^2-y^2}]$  and  $\Delta_2(\mathbf{k})[d_{xy}]$  by  $\Delta_1 \cos(2\phi)$  and  $\Delta_2 \sin(2\phi)$  respectively:

$$\hat{\Delta} = \Delta_1 \cos(2\phi) \alpha_3 + \Delta_2 \sin(2\phi) \alpha_1, \quad (\text{S2})$$

where the  $\cos(2\phi)$  and  $\sin(2\phi)$  stand for effective  $d_{x^2-y^2}$  and  $d_{xy}$  form factors respectively. The effective gap is then given by  $|\hat{\Delta}|^2$ , which, in view of the anti-commutation of the Pauli matrices, reproduces the expression given in the main text. For  $\text{CeCu}_2\text{Si}_2$ , the analogue of Fig. 1 of Ref. 36 is given in Fig. 4 of the main text.

Finally, we note that  $s\tau_3$  is one of the pairing states driven by magnetic fluctuations. Indeed, in the microscopic models for the Fe-based SCs in which unconventional superconductivity is induced for short-range spin-exchange interactions, the phase diagram for the superconducting pairing state was studied in Ref. 36. It was shown that the  $s\tau_3$  pairing is stabilized over an extended region of the phase diagram. It is worth underscoring that the entire pairing function in (S1) – as opposed to the individual  $\Delta_1(\mathbf{k})[d_{x^2-y^2}] \alpha_3$  intraband or  $\Delta_2(\mathbf{k})[d_{xy}] \alpha_1$  interband component – describes this pairing state. This property carries over to the case of (S2) proposed for  $\text{CeCu}_2\text{Si}_2$ . Thus, the entire pairing function corresponds to a single pairing channel and, in particular, the intra-band and interband components admit no linear coupling and will have the same temperature dependence.

In short, the minimal  $d+d$  multiband pairing provides a simple scenario which can in principle reconcile seemingly contradictory experimental signatures. In particular, it provides a good fit to the observed penetration depth and superfluid-density measurements.

### Fitting the low temperature penetration depth

The temperature dependence of the London penetration depth shift  $\Delta\lambda(T) = \lambda(T) - \lambda(0)$  was analyzed using both a model for a fully gapped superconductor and a power law relationship  $\sim T^n$ , as described in the main text. The fitting with the power law was performed from the base temperature of 40 mK up to a temperature  $T_{up}$ , and the dependence of the exponent  $n$  on  $T_{up}$  was obtained. The data were fitted using a standard weighted least squares method. The weights were given by  $1/\sigma_i^2$ , where  $\sigma_i$  is the uncertainty of the  $i^{\text{th}}$  data point. Since a large number of datapoints were measured for TDO,  $\sigma_i$  were estimated from the standard deviation of the data within narrow temperature intervals.



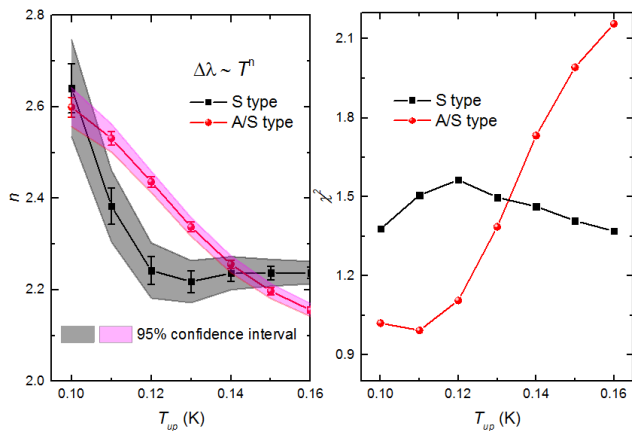


FIG. S1. The dependence of the exponent  $n$  on  $T_{up}$  upon fitting  $\Delta\lambda(T)$  with a  $\sim T^n$  dependence for both samples. The shaded areas show the area enclosed by the 95% confidence intervals. (b) The dependence of the goodness of fit  $\chi^2$  on  $T_{up}$  for both samples.

The dependence of the exponent  $n$  on  $T_{up}$  is displayed in Fig. S1(a). For both samples there is an increase of  $n$  with decreasing temperature, with an exponent significantly larger than two. The shaded areas illustrate the 95% confidence intervals, showing that there is a high level of confidence that the exponent is greater than two at low temperatures. This is clear evidence for nodeless superconductivity. The goodness of fit,

$$\chi^2 = \frac{1}{N} \sum_{i=1}^N (\lambda_i - \lambda_{fit})^2 / \sigma_i^2, \quad (\text{S3})$$

for the fits of the power law behavior is displayed in Fig. S1(b), where  $\lambda_i$  are the experimental datapoints,  $\lambda_{fit}$  are the calculated model values and  $N$  is the number of degrees of freedom ( $\approx$  number of datapoints). At low temperatures  $\chi^2$  is close to one, indicating the data are well described by an exponent larger than two, but there is no evidence that the model overfits the data.